SPE 142884

A Unified Mathematical Model for Unconventional Reservoir Simulation

Yu-Shu Wu and Perapon Fakcharoenphol, Colorado School of Mines

This paper was prepared for presentation at the SPE EUROPEC/EAGE Annual Conference and Exhibition held in Vienna, Austria, 23–26 May 2011.

Abstract

Unconventional hydrocarbon resources from low-permeability formation, i.e., tight sands and shales, are currently received great attention because of their potential to supply the entire world with sufficient energy for the decades to come. In the past few years, as a result of industry-wide R&D effort, progresses are being made towards commercial development of gas and oil from such unconventional resources. However, studies, understandings, and effective technologies needed for development of unconventional reservoirs are far behind the industry needs.

Unconventional reservoir dynamics is characterized by highly nonlinear behavior of multiphase flow in extremely low-permeability rock, coupled by many co-existing, processes, e.g., non-Darcy flow and rock-fluid interaction within tiny pores or micro-fractures. Quantitative characterization of unconventional reservoirs has been a significant scientific challenge currently. Because of complicated flow behavior, strong interaction between fluid and rock as well as multi-scaled heterogeneity, the traditional Darcy-law-and-REV-based model may not be applicable for describing flow phenomena in unconventional reservoirs. In this paper, we will discuss a general mathematical model proposed for unconventional reservoir simulation. We will present a unified framework model to incorporate various nonlinear flow and transport processes using a multi-domain, multi-continuum concept to handle multi-scaled heterogeneity of unconventional formation. Specifically, we will use extended or modified Darcy law to include the following processes: (1) non-Darcy flow with inertial effects; (2) non-Newtonian behavior (i.e., threshold pressure gradient for flow to occur); (3) adsorption and other reaction effect; and (4) rock deformation. The proposed modeling methodology has been implemented into a general reservoir simulator and will be demonstrated for its application in analyzing well tests in fractured vuggy reservoirs, non-Darcy flow, and non-Newtonian flow in porous and fractured reservoirs.

Introduction

Significant progress has been made in the past decade in producing gas and oil from unconventional petroleum resources, including low-permeability shale oil and gas reservoirs, and tight gas formations. However, low gas/oil recovery rate from such unconventional resources remains as the main technical difficulty. For example, gas recovery rate from these unconventional resources is estimated at 10-30% of GIP, much lower from conventional gas reservoirs. Gas and oil production or flow in such extremely low-permeability formations is complicated by flow condition and many co-existing processes, such as severe heterogeneity, Klinkenberg effect (Klinkenberg, 1941), non-Darcy flow behavior, adsorption/desorption, strong interactions between fluids (gas and water) molecules and solid materials within tiny pores, as well as micro- and macro- fractures of shale and tight formations. Currently, there is little in basic understanding on how these complicated flow behavior impacts on gas flow and the ultimate gas recovery from such reservoirs. There is a general lack in technologies or approaches available for effective gas production from unconventional reservoirs (MIT, 2010), except two technologies: horizontal drilling and hydraulic fracturing, which seems to work (Denny, 2008; Bybee, 2008; King, 2010). In particular, there are no effective and applicable reservoir

simulators currently available and few modeling efforts (Kelkar and Atiq, 2010) in the industry for assisting engineers to model and develop the unconventional natural gas resources.

Currently, there are no effective reservoir simulators or modeling approaches available for engineers to use in developing unconventional shale gas or tight reservoirs (MIT, 2010). The common practice in field application is either using no simulation tools at all or using Darcy's law based commercial reservoir simulators for scope calculations with many overly simplified assumptions. Therefore, there is a need to develop and use a realistic modeling tool for petroleum engineers in developing unconventional natural gas resources. Flow behavior in shale oil/gas and tight gas reservoirs is characterized by two-phase (oil and brine, or gas and liquid) flow in extremely low-permeability, highly heterogeneous porous/fractured, and stress-sensitive rock. Because of the low permeability in such shale or tight rock, the traditional, Darcy's law based simulators will not be applicable or realistic to handling nonlinearity of such flow. For example, the traditional double-porosity model may not be suitable for handling fracture-matrix interaction of gas flow in these reservoirs, because of the long-last transient nature of fracture-matrix interaction from the extremely low-permeability rock, because of the time scale to reach pseudo-statedy flow condition between fractures and the matrix. In addition to the need of general capability of modeling multiple-scale heterogeneous porous or fractured formations, the physical processes of gas adsorption, desorption onto solids grain or organic matter, as well as diffusion into flow streams, are in general not described in existing commercial petroleum reservoir simulators.

This paper presents a unified mathematical model for simulating both oil and gas flow and production processes in shale oil/gas and tight gas reservoirs. To describe oil/gas flow behavior in low-permeability, highly heterogeneous porous or (natural or man-made) fractured, and stress-sensitive shale oil/gas and tight gas reservoirs, a generalized mathematical model is proposed to incorporate all the key relevant physical processes, i.e., nonlinear and non-Darcy flow, Klinkenberg effect, and coupled fluid flow and rock deformation, as well as diffusion, and sorption phenomena. The proposed mathematical model has been tested using a multiphase, multidimensional reservoir simulator (Wu, 2000). The proposed numerical modeling approach is suitable for modeling various types of shale and gas reservoirs, including discrete- hybrid- double-, and other multiple-continuum conceptual models for multi-scaled fractures and matrix systems and flow domains. The simulator can be used for quantitative studies of unconventional reservoir dynamics and performance, fractures and their effects on oil or gas production, well and stimulation design, and optimal production schedules in the field. As a domenstraion example, the simulator is used to simulate oil production from a complicated hydraulic and natural fracture network coupled with rock deformation in a shale oil reservoir using a hybrid fracture model.

Mathematical Framework Model

The unconventional oil/gas reservoir simulator to be developed will couple multiphase fluid flow and mass diffusion with effect of rock deformation and chemical reaction of adsorption and desorption processes in unconventional reservoirs. In numerical formulation, the integral finite difference method (Pruess et al. 1999) will be used for space discretization of multidimensional fluid and heat flow in porous and fractured reservoirs using an unstructured/structured grid. Time will be discretized fully implicitly as a first-order backward finite difference. Time and space discretization of mass balance equations results in a set of coupled non-linear equations, to be solved fully implicitly using Newton iteration.

Multi-continuum approaches to be implemented include the classical double-porosity model, the more rigorous dual-continuum generalization of the MINC, and the multi-continuum model (Kazemi, 1969; Pruess and Narasimhan, 1985; Wu and Pruess, 1988). The general multi-continuum modeling approach is also able to handle discrete-fracture model and hybrid grids of combining discrete-fracture, multicontinuum-, and single-continuum models (Wu and Qin, 2009). The proposed mathematical model is tested based on the multiphase, multidimensional reservoir simulator of MSFLOW (Wu, 2000).

A generalized conservation equation of mass components in a multiphase, isothermal porous or fractured system, consisting of multiple mass components (C_nH_{2n+2}, H_2O, etc.), is written,

$$\frac{\partial M^k}{\partial t} = q^k + F^k + R^k \tag{1}$$

where superscript k is the index for components, k = 1, 2, 3,…, N_c, with N_c being the total number of mass components; M^k is the accumulation term of component k in all phases and solids; q^k is a source/sink term or fracture-matrix exchange term for

component $\underline{k}$; R^k is a reaction representing mass reaction from solid phases such as adsorption, dissolution and precipitation for component k; and F^k is the "flow" or transport term of net mass movement or net exchange from multiphase flow and transport. The mass transport is in general governed by processes of advection, diffusion, and dispersion, and is also subject to other processes such as adsorption and partitioning between phases, and may be described as,

$$F^k = -\sum_\beta \nabla \bullet \left(\rho_\beta X_\beta^k \mathbf{v}_\beta\right) + \sum_\beta \nabla \bullet \left(\underline{D}_\beta^k \bullet \nabla\left(\rho_\beta X_\beta^k\right)\right) \qquad (k = 1, 2, 3, \ldots, N_c) \tag{2}$$

where X_β^k is the mass fraction of component k in fluid β; ρ_β is the density of fluid β; $\mathbf{v}_\beta$ is the flow velocity, as defined below, for different flow regimes, $\underline{D}_\beta^k$ is the hydrodynamic dispersion tensor accounting for both molecular diffusion and mechanical dispersion for component k in phase β, defined by an extended dispersion model to include multiphase effect and fracture-matrix interaction (Wu and Pruess, 2000).

The velocity in Eq. (2) will evaluated (1) using the Darcy's law with Klinkenberg effects (for gas flow); (2) using the nonlinear flow models to describe non-Darcy flow behavior (e.g., Wu, 2002) and (3) conditions where flow may not occur until the pressure or potential gradient reaches a certain threshold value (Wu and Pruess, 1998). In addition, stress-sensitive shale gas and tight-gas formation is handled using the coupled modeling approaches with observation and experimental results (Wu et al. 2008) and previous research (Rutqvist et al. 2002), in which the effective porosity, permeability, and capillary pressure of rock, in particular, for multi-scaled fractures, are assumed to correlate with the mean effective stress.

$\mathbf{v}_\beta$ is the flow velocity (or volumetric flow rate) in Eq. (2), defined differently under different flow regimes or situations, as discussed in the following.

Darcy's Flow: When the Darcy's law is applicable, the velocity, $\mathbf{v}_\beta$, is defined as,

$$\mathbf{v}_\beta = -\frac{k k_{r\beta}}{\mu_\beta}\left(\nabla \Phi_\beta\right) \tag{3}$$

where k is the absolute/intrinsic permeability of the formation, treated as a function of effective stress for stress sensitive reservoirs or pressure with Klinkenberg effect; $k_{r\beta}$ is relative permeability to phase β, treated as a function of fluid saturation; μ_β is the viscosity of phase β as a function of pressure; and $\nabla\Phi_\beta$ is flow potential gradient, defined as,

$$\nabla \Phi_\beta = \left(\nabla P_\beta - \rho_\beta g \nabla D\right) \tag{4}$$

where P_β is the pressure of phase β; g is gravitational acceleration; and D is the depth from a datum.

Non-Darcy's Flow: In addition to multiphase Darcy flow, non-Darcy flow may also occur between and among the continua in tight gas reservoirs. The flow velocity, $\mathbf{v}_\beta$, for non-Darcy flow of each fluid may be described using the multiphase extension of the *Forchheimer* equation (e.g., Wu, 2002),

$$-\left(\nabla \Phi_\beta\right) = \frac{\mu_\beta}{k_{r\beta}} k \mathbf{v}_\beta + \beta_\beta \rho_\beta \mathbf{v}_\beta \left|\mathbf{v}_\beta\right| \tag{5}$$

where β_β is the effective non-Darcy flow coefficient with a unit m^{-1} for fluid β under multiphase flow conditions.

Non-Newtonian Flow: Non-Newtonian flow is used in this work to describe conditions where flow may not occur until the pressure or potential gradient reaches a certain threshold value, which is similar to Bingham non-Newtonian fluid flow in porous media. Such a threshold-pressure-gradient concept is commonly used to describe nonlinear flow behavior in low permeability reservoirs (Xiong et al. 2008; Lei et al. 2007). Instead of introducing an apparent viscosity for Bingham fluid, an effective potential gradient approach, as follows, has been proven to be more efficient numerically (Wu et al., 1992). Using the effective potential gradient, the flow of gas or liquid in a low-permeability reservoir is described by,

$$\mathbf{v}_\beta = -\frac{kk_{r\beta}}{\mu_\beta}\left(\nabla\Phi_e^\beta\right) \tag{6}$$

where $\mu_{b,\beta}$ is the Bingham plastic viscosity coefficient for phase β; and $\nabla\Phi_e^\beta$ is the effective potential gradient whose scalar component in the x direction (the flow direction) is defined as,

$$\left(\nabla\Phi_e\right)_x = \left(\nabla\Phi\right)_x - G \quad \text{for} \quad \left(\nabla\Phi\right)_x > G \tag{7a}$$

$$\left(\nabla\Phi_e\right)_x = \left(\nabla\Phi\right)_x + G \quad \text{for} \quad \left(\nabla\Phi\right)_x < -G \tag{7b}$$

$$\left(\nabla\Phi_e\right)_x = 0 \quad \text{for} \quad -G < \left(\nabla\Phi\right)_x < G \tag{7c}$$

where G is the threshold (or minimum) potential gradient for the fluid to become mobile.

Coupled fluid flow and geomechanics: geomechanics play an important role in development of unconventional resources. During a hydraulic fracturing, the stresses at close vicinity to the well are alternated by both fracture face displacement and pore pressure change. Consequently, they may activate natural fractures and therefore open microflow channels in the drainage area of stimulated wells. Furthermore, during the production period, pressure decreasing induces change in effective stresses. As a result, the width and permeability of micro channels are altered. To capture such an effect, we fully couple geomechanics to fluid flow modules. The inherent assumptions for the development of the geomechanics module are listed as follows:

- Rock mechanics properties are isotropic
- Rock behaves as a perfectly elastic media (linear, reversible and non-retarded mechanical behavior)
- Rock deformation are relatively small and can accurately compute using small strains assumption;
- Lateral deformation of rock frame is negligible compare to vertical displacement (uniaxial strain)

Although the fracture face displacement typically occurs in lateral directions, it only affects early production performance by activating natural fractures. While, we assumed that the area of activated natural fracture is known from microseismic data, long term production performance, dominated by pressure induced stress changes, can be calculated. Under uniaxial strain assumption, stress changes can be expressed as

$$\sigma'(x,y,z,P) = \sigma(x,y,z,P) - \alpha P \tag{8}$$

$$\Delta\sigma'_z(x,y,z,P) = -\alpha\Delta P \tag{9}$$

$$\Delta\sigma'_x(x,y,z,P) = \Delta\sigma'_y(x,y,z,P) = -\frac{\nu}{(1-\nu)}\alpha\Delta P \tag{10}$$

$$\varepsilon_z = -\alpha_P \Delta P \frac{(1+\nu)(1-2\nu)}{E(1-\nu)} \tag{11}$$

where σ' is effective stress (psi), $\Delta\sigma'_x$ is effective stress change in x-direction (psi), $\Delta\sigma'_y$ is effective stress change in y-direction (psi), $\Delta\sigma'_z$ is vertical effective stress change (psi), ε_z is vertical strain where ε_z=0 at the initial condition, ΔP is pressure change (psi) defined as ($P - P_i$), α is Biot constant, ν is Poisson ratio, and E is elastic modulus (psi).

Note that, Eqs. (9) – (11) are fully coupled to fluid flow model. The scheme does not require additional primary variable, as such minimum computational load is required.

Stress-Sensitive Formation: Based on the observation from experimental results (e.g., Xiong et at. 2008; Wu et al. 2008) and previous research (Terzaghi, 1943; Rutqvist et al. 2002), the effective porosity, permeability, and capillary pressure of rock are assumed to correlate with the mean effective stress (σ'_m) as,

$$\sigma_m(x,y,z,P) = (\sigma_x(x,y,z,P) + \sigma_y(x,y,z,P) + \sigma_z(x,y,z,P))/3 \tag{9}$$

where σ_x, σ_y, and σ_z are total stress in x, y, and z- directions, respectively.

With the definition of the mean effective stress in Eq. (8), the effective porosity of formation is defined as a function of mean effective stress only,

$$\phi = \phi(\sigma'_m) \tag{10}$$

Similarly, the intrinsic permeability is related to the effective stress, i.e.,

$$k = k(\sigma'_m) \tag{11}$$

For capillary-pressure functions, the impact of rock-deformation or pore-change is accounted for using the Leverett function (Leverett, 1941),

$$P_c = C_p P_c^0(S_w) \frac{\sqrt{k^0/\phi^0}}{\sqrt{k(\sigma'_m)/\phi(\sigma'_m)}} \tag{12}$$

where P_c is the capillary pressure between gas and water as a function of water or gas saturation; C_p is a constant; and the superscript 0 denotes reference or zero-stress condition.

A conceptual model consisting of cubic blocks is used to characterize a highly fractured system. Flow in this system occurs through the apertures between blocks, and changes in the three-dimensional stress field cause these apertures to change width.

$$w_f = w_f(\sigma'_n) \tag{13}$$

where w_f is fracture aperture (μm) and σ_n' is effective normal stress to fracture plane. Porosity and permeability correction factors can be calculated from aperture changes.

$$\phi_f = \phi_f(w_{fx}, w_{fy}, w_{fz}) \tag{14}$$

where ϕ_f is fracture porosity, w_{fx} ,w_{fy} ,w_{fz} are fracture widths in direction perpendicular to x, y, and z direction.

$$k_{fx} = k_{fx}(w_{fy}, w_{fz}) \qquad k_{fy} = k_{fx}(w_{fx}, w_{fz}) \qquad k_{fz} = k_{fx}(w_{fx}, w_{fy}) \tag{15}$$

To incorporate rock-deformation effects at a given site, the proposed model correlations, Eqs. (10), (11), (12), and (13), need to be determined from laboratory or field studies. The key for applicability of these models in multiphase flow simulations coupled with rock deformation is that the distribution of effective stress or total stress field must be predetermined as a function of spatial coordinates and pressure fields, as in Eqs. (8) - (10). In practice, the stress distribution may be estimated analytically, numerically, or from field measurements, because changes in effective stress are primarily caused by changes in reservoir pressure. These models can be significantly simplified for coupling multiphase gas flow with rock deformation in stress-sensitive formations in numerical simulation, if the *in situ* total stress in reservoirs is constant or a function of spatial coordinates as well as fluid pressure.

Klinkenberg Effect: In low-permeability formation or under low pressure condition, the Klinkenberg effect may be too significant to be ignored when modeling gas flow in reservoirs (Wu et al. 1998). Under such flow conditions, absolute permeability for the gas phase is written as a function of gas pressure as,

$$k_g = k_\infty \left(1 + \frac{b}{P_g}\right) \tag{16}$$

where k_∞ is constant, absolute gas-phase permeability under very large gas-phase pressure (where the Klinkenberg effect is minimized); and b is the Klinkenberg factor, depending on the pore structure of the medium and formation temperature.

Fracture Flow Conceptual Model: Handling highly anisotropic fractures and multiple scale of heterogeneity in fractures of shale/tight formations is the key of unconventional reservoir simulators, because the success of any production scenarios in shale oil/gas and tight gas reservoirs depends on (1) how to enhance oil/gas flow through hydraulic or nature fractures and (2) how to handle mass transfer between different-scaled, fracture-matrix (including micro-fractures), and pore and flow domains. We implement a general fracture conceptual model for modeling various types of fractures and model domains in shale and tight oil/gas reservoirs, including discrete- hybrid- double-, and other multiple-continuum conceptual models for multi-scaled fractures and matrix systems and flow/rock domains. The technique used in developing and implementing general fracture conceptual models to simulating fluid and heat flow processes in fractured unconventional reservoirs follows a generalized dual-continuum methodology (Kazemi, 1969; Pruess and Narasimhan, 1985; Wu and Pruess, 1988; Wu and Qin, 2009). This method treats fracture and matrix flow and interactions using a multi-continuum numerical approach, including the double- or multiporosity method, the dual-permeability method, and the more general MINC method (Pruess and Narasimhan, 1985). It has been shown (e.g., Wu et al. 2004) that the same continuum concept is also applicable to multiphase flow though single or multiple discrete fractures, hydird grid, or fracture network.

Numerical Formulation

The methodology for using numerical approaches to simulate multiphase flow and transport in unconventional reservoirs consists in general of the following three steps: (1) spatial discretization of mass conservation equations; (2) time discretization; and (3) iterative approaches to solve the resulting nonlinear, discrete algebraic equations.

Discrete Equations: The component mass-balance Equations (Eq.1) are discretized in space using a control-volume or integrated finite difference concept, as shown in **Fig. 1**. The control-volume approach provides a general spatial discretization scheme that can represent a one-, two- or three-dimensional domain using a set of discrete meshes. Each mesh has a certain control volume for a proper averaging or interpolation of flow and transport properties or thermodynamic variables. Time discretization is carried out using a backward, first-order, fully implicit finite-difference scheme. The discrete nonlinear equations for components of water, gas and oil at gridblock or node i can be written in a general form:

$$\left\{M_i^{k,n+1} - R_i^{k,n+1}\Delta t - M_i^{k,n}\right\}\frac{V_i}{\Delta t} = \sum_{j\in\eta_i} \text{flow}_{ij}^{k,n+1} + Q_i^{k,n+1} \tag{17}$$

$(k = 1, 2, 3, \ldots, N_c)$ and $(i=1, 2, 3, \ldots, N)$

where superscript k serves also as an equation index for all mass components with $k = 1, 2, 3, \ldots, N_c$; superscript n denotes the previous time level, with n+1 the current time level to be solved; subscript i refers to the index of gridblock or node i, with N being the total number of nodes in the grid; Δt is time step size; V_i is the volume of node i; η_i contains the set of direct neighboring nodes (j) of node i; M_i^k, R_i^k, flow_{ij}^k, and Q_i^k are the accumulation and reaction (decay/generation, asorption, or desorption) terms, respectively, at node i; the component mass "flow" term between nodes i and j, and sink/source term at node i for component k, respectively, defined below.

The "flow" terms in Eq. (17) are generic and include mass fluxes by advective and dispersive processes, as described by Eq. (2). The phase mass flow term of Eq. (17) for multiphase flow is described by a discrete version of Darcy's law, i.e., the mass flux of fluid phase β along the connection is given by

$$\text{flow}_{ij}^k = \sum_\beta \left(X_{\beta,ij+1}^k \text{flow}_{\beta,ij}\right) \tag{18a}$$

and

$$\text{flow}_{\beta,ij} = \lambda_{\beta,ij+1/2}\gamma_{ij}\left(\Phi_{\beta j} - \Phi_{\beta i}\right) \tag{18b}$$

where $\lambda_{\beta,i\,j+1/2}$ is the mobility term to phase β, defined as

$$\lambda_{\beta,i\,j+1/2} = \left(\frac{\rho_\beta k_{r\beta}}{\mu_\beta}\right)_{ij+1/2} \tag{19}$$

In Eq. (18b), γ_{ij} is transmissivity and is defined differently for finite-difference or finite-element discretization. If the integral finite-difference scheme (Pruess et al. 1999) is used, the transmissivity is evaluated as,

$$\gamma_{ij} = \frac{A_{ij} k_{ij+1/2}}{D_i + D_j} \tag{20}$$

where A_{ij} is the common interface area between the connected blocks or nodes i and j; D_i is the distance from the center of block i to the common interface of blocks i and j; and $k_{ij+1/2}$ is an averaged (such as harmonic-weighted) absolute permeability along the connection between elements i and j. The flow potential term in Eq. (18b) is defined as,

$$\Phi_{\beta i} = P_{\beta i} - \rho_{\beta,ij+1/2}\, g\, Z_i \tag{21}$$

where Z_i is the depth to the center of block i from a reference datum.

Handling fractured media: to implement all fractured modeling approaches, special attention is needed to calculate fracture-matrix mass transfer where a quasi-steady state is assumed e.g. in double-porosity, dual-permeability. The flow between fractures and matrix is still evaluated using Eq. (18b); however, the transmissibility for the fracture-matrix flow is given by,

$$\gamma_{ij} = \frac{A_{FM} k_M}{l_{FM}} \tag{22}$$

where A_{FM} is the total interface area between fractures and matrix of element i and j (one of them is a fracture and the other is a matrix blocks); k_M is a matrix absolute permeability; and $\boldsymbol{l}_{FM}$ is a characteristic distance representing an equivalent length of average matrix block pressure for a quasi-steady state flow. It can be calculated from ideal one-, two, and three-dimensional rectangular matrix block.

Handling Klinkenberg effects: To include the Klinkenberg effect on gas flow, the absolute permeability to gas phase in (17) should be evaluated using Eq. (16), as a function of gas phase pressure.

Handling rock deformation effects: If the stress field is predetermined or estimated numerically as a function of spatial coordinates and fluid pressure, the effect of rock deformation on fluid flow can be evaluated using Eq. (10) and (14) for porosity, Eq. (11) and (15) for absolute permeability, and Eq. (12) for capillary pressure, respectively, as functions of effective stress and other primary and secondary variables in numerical formulation.

Handling "non-Newtonian" flow: In the case that gas or water flow is subject to a threshold potential gradient, the discrete potential gradient in (18b) should be replaced by the effective potential gradient, Eq. (7) for phase flow term evaluation.

Handling non-Darcy flow: Under the non-Darcy flow condition of Eq. (5), the flow term ($\text{flow}_{\beta,ij}$) in Eq. (18) along the connection (i, j), between elements i and j, is numerically defined as (Wu, 2002),

$$\text{flow}_{\beta,ij} = \frac{A_{ij}}{2\left(k\beta_\beta\right)_{ij+1/2}}\left\{-\frac{1}{\lambda_\beta}+\left[\left(\frac{1}{\lambda_\beta}\right)^2-\bar{\gamma}_{ij}\left(\Phi_{\beta j}-\Phi_{\beta i}\right)\right]^{1/2}\right\} \tag{23}$$

in which the non-Darcy flow transmissivity is defined as,

$$\bar{\gamma}_{ij} = \frac{4\left(k^2\rho_\beta\beta_\beta\right)_{ij+1/2}}{d_i+d_j} \tag{24}$$

Note that Eq. (17), a discrete equation of mass conservation, has the same form regardless of the dimensionality of the model domain, i.e., it applies to one-, two-, or three-dimensional analyses of flow through porous or fractured media.

For mass component transport, the "flow" term or the net mass flux by advection and hydrodynamic dispersion of a component along the connection of nodes i and j, is determined by

$$\text{flow}_{ij}^k = F_{A,ij}^k + F_{D,ij}^k \quad (k = 1, 2, 3, \ldots, N_c) \tag{25}$$

where $F_{A,ij}^k$ and $F_{D,ij}^k$ are the net mass fluxes by advection and hydrodynamic dispersion along the connection, respectively, with

$$F_{A,ij}^k = A_{ij}\sum_\beta\left(X_\beta^k\right)_{ij+1/2}\text{flow}_{\beta,ij} \tag{26}$$

and

$$F_{D,ij}^k = -\mathbf{n}_{ij}\bullet A_{ij}\sum_\beta \underline{D}_\beta^k \bullet \nabla\left(\rho_\beta X_\beta^k\right) \tag{27}$$

where $\mathbf{n}_{ij}$ is the unit vector along the connection of the two blocks i and j.

In evaluating the "flow" terms in the above Eqs. (17)-(27), subscript ij+1/2 is used to denote a proper averaging or weighting of fluid flow, component transport, or heat-transfer properties at the interface or along the connection between two blocks or nodes i and j. The convention for the signs of flow terms is that flow from node j into node i is defined as "+" (positive) in calculating the flow terms.

Note that we present explicit, discrete expressions for estimating all the flow terms above, except for dispersive fluxes in Eq. (25). This is because of the numerical difficulties introduced in handling the hydrodynamic tensor of dispersion, which is treated very differently with different numerical approaches, such as finite difference or finite element. In most formulations for solute transport, the off-diagonal terms and contributions of the dispersion tensor are ignored, and dispersive transport is considered only along the principal directions. However, a general procedure for using the integral finite difference to incorporate a full dispersion tensor is presented by Wu and Pruess (2000).

Eq. (17) presents a precise form of the balance equation for each mass component and heat in a discrete form. It states that the rate of change in mass accumulation (plus decay/generation, adsorption or desorption, if existing) at a node over a time step is exactly balanced by inflow/outflow of mass, and also by sink/source terms, when existing for the node. As long as all flow terms have flow from node i to node j equal to and opposite to that of node j to node i for fluids, components, and heat, no mass will be lost or created in the formulation during the solution. Therefore, the discretization in Eq. (17) is conservative.

Numerical Solution Scheme

There are a number of numerical solution techniques that have been developed in the literature over the past few decades to solve the nonlinear, discrete equations of reservoir simulations. When handling multiphase flow and multicomponent transport in a multiphase flow system, the predominant approach is to use a fully implicit scheme. This scheme is best because of the extremely high nonlinearity inherent in those discrete equations and the many numerical schemes with different level of explicitness that fail to converge in practice. In this section, we discuss a general procedure to solve the discrete nonlinear Eq. (17) fully implicitly, using a Newton iteration method.

Let us write the discrete nonlinear Eq. (17) in a residual form as,

$$R_i^{k,n+1} = \left\{M_i^{k,n+1} + \Delta t R_i^{k,n+1} - M_i^{k,n}\right\}\frac{V_i}{\Delta t} - \sum_{j\in\eta_i} flow_{ij}^{k,n+1} - Q_i^{k,n+1} = 0 \tag{28}$$

($k = 1, 2, 3, \ldots, N_c$; $i = 1, 2, 3, \ldots, N$).

Eq. (28) defines a set of $(N_c) \times N$ coupled nonlinear equations that need to be solved for every balance equation of mass components, respectively. In general, (N_c) primary variables per node are needed to use the Newton iteration for the associated (N_c) equations per node. The primary variables are usually selected among fluid pressures, fluid saturations, and mass (mole) fractions of components in fluids. In many applications, however, primary variables cannot be fixed and must be allowed to vary dynamically to deal with phase appearance and disappearance (Forsyth, 1994). The rest of the dependent variables, such as relative permeability, capillary pressures, viscosity and densities, partitioning coefficients, and dispersion tensor, as well as nonselected pressures, saturations, and mass (mole) fractions—are treated as secondary variables, which are calculated from selected primary variables.

In terms of the primary variables, the residual equation, Eq. (28), at a node i is regarded as a function of the primary variables at not only node i, but also at all its direct neighboring nodes j. The Newton iteration scheme gives rise to

$$\sum_m \frac{\partial R_i^{k,n+1}\left(x_{m,p}\right)}{\partial x_m}\left(\delta x_{m,p+1}\right) = -R_i^{k,n+1}\left(x_{m,p}\right) \tag{29}$$

where x_m is the primary variable m with $m = 1, 2, 3, \ldots, N_c$, respectively, at node i and all its direct neighbors; p is the iteration level; and $i = 1, 2, 3, \ldots, N$. The primary variables in Eq. (29) need to be updated after each iteration,

$$x_{m,p+1} = x_{m,p} + \delta x_{m,p+1} \tag{30}$$

The Newton iteration process continues until the residuals $R_n^{k,n+1}$ or changes in the primary variables $\delta x_{m,p+1}$ over an iteration are reduced below preset convergence tolerances.

Numerical methods are generally used to construct the Jacobian matrix for Eq. (29), as outlined in Forsyth et al. (1995). At each Newton iteration, Eq. (29) represents a system of $(N_c) \times N$ linearized algebraic equations with sparse matrices, which are solved by a linear equation solver.

Treatment of Initial and Boundary Conditions: A set of initial conditions is required to start a transient simulation, i.e., a complete set of primary variables need to be specified for every gridblock or node. A commonly used procedure for specifying initial conditions is the restart option, in which a complete set of initial conditions or primary unknowns is generated in a previous simulation, with proper boundary conditions described.

Because of more physical and chemical constraints, boundary conditions for a multiphase flow and transport problem are generally much more difficult to handle than for a single-phase situation. When using a block-centered grid, first-type or Dirichlet boundary conditions can be effectively treated with the “inactive cell” or “big-volume” method, as normally used in the TOUGH2 code (Pruess et al. 1999). In this method, a constant pressure/saturation/concentration/temperature node is specified as an inactive cell or with a huge volume, while keeping all the other geometric properties of the mesh unchanged. With finite-element or edge-centered finite-difference grids, first-type boundary conditions and Neuman boundary conditions can be treated using a generalized, sink/source term approach(Wu et al. 1996). Description of more general types of flux or mixed boundaries, such as bottom water drive and multilayered wells of production or injection, is part of the solution, and general procedures for handling such boundary conditions are discussed in Wu et al. (2000; 1996).

Application

In this section, we demonstrate the use of the proposed mathematical model for modeling oil production from a shale oil reservoir associated with hydraulic fracturing. The stress alteration induced by hydraulic fracturing activates existing natural fractures, and therefore opens microflow channels in the drainage area of stimulated wells. Seismic data collected in unconventional reservoirs has indicated that the stimulated areas are much larger than a simple planar fracture could create. Here we present the simulation of a hydraulic fracturing problem as an example case to illustrate the capability of our hybrid fracture model to capture such the complex fracture network in these reservoirs. **Fig. 2** shows the schematic of the level of fracture complexities (Warpinski et al., 2008).

The system we modeled includes a single vertical hydraulic fracture in the drainage area of a well in a 3-D setting. A shale oil reservoir is divided into two natural fractured areas–active and non-active, **Fig. 3**. Fluids in the system include oil and water. The same vertical well is used for both injection and production depending on the stage of the hydraulic fracturing process.

To simulate performance of this system using our model, the hydraulic fracture is represented by the discrete fracture model, an active naturally-fractured reservoir area is described by the continuum fracture model, while a non-active natural fractured reservoir area is represented by the single-porosity model. Since the system is symmetric, only a quarter of this hydraulically fractured reservoir system is modeled (**Fig. 4)**. The basic parameter set for the simulation is summarized in **Table 1.**

Figs. 5 shows the permeability map in the drainage area of the well both before and after a hydraulic fracturing treatment, respectively. An increase in pore pressure around the hydraulic fracture causes significant reduction in the effective stresses, potentially reopening the existing healed natural fractures or creating new fractures. As a result, the permeability near the well of the reservoir is significantly improved. This effect would help increase the well performance in the initial production. However, the long-term well performance depends on the behavior of these opened natural fractures. If these fractures are not fully closed when pressure drop below the initial pressure, which is typically the case due to the roughness of the face of the natural fractures, we could see significant improvement in production as shown in **Fig. 6.**

Summary and Concluding Remarks

In this paper, we present a unified mathematical model for oil or gas flow in unconventional, low-permeability porous or fractured reservoirs of shales or tight formations. To describe gas flow behavior in such low-permeability, highly heterogeneous porous or fractured, and stress-sensitive rock, the model formulation incorporates many relevant physical processes, i.e., Klinkenberg effect, non-Newtonian behavior, non-Darcy flow with inertial effect, and coupled rock deformation with multiphase fluid flow. The proposed mathematical model has been implemented and tested using a multiphase, multidimensional reservoir simulator. The numerical implementation of the unified formulation is based on a control-volume spatial discretization, using an unstructured grid, and the time discretized with a fully implicit finite-difference method. The final discrete linear or nonlinear equations are handled fully implicitly, using Newton iteration.

The proposed numerical modeling approach, based on a general multiple-continuum concept, is suitable for modeling various types of fractured or porous reservoirs, including double-, triple-, and other multiple-continuum conceptual models for multi-scaled fractures and matrix systems. The proposed general modeling methodology is demonstrated for its application in the example case where oil production is simulated using a hybrid, discrete-fracture, double-porosity, and single-porosity model from a low permeability, hydraulic fractured shale oil reservoir. The model application to actual shales or tight gas reservoirs is an on-going research project and will be reported in the future.

Acknowledgments

This work was supported in part by Colorado School of Mines and by Sinopec Inc. of China through "National Basic Research Program of China (2006CB202400)."

Nomenclature

A_{ij}	interface areas between two gridblock i and j (m^2)
b	Klinkenberg factor (Pa)
D	depth from a datum, m
$flow_{\beta,ij}$	mass flow of fluid β ($kg/s/m^2$) along connection ij of time level n+1

$flow^{k}_{\beta,ij}$	mass flow of component k in fluid β (kg/s/m^2) along connection ij of time level n+1
g	gravitation constant (m/s^2)
G	threshold pressure or potential gradient (Pa/m)
k	absolute permeability of porous media (m^2)
$k_{r\beta}$	relative permeability to phase β
k_{∞}	absolute permeability at large gas pressure
P	Pressure (Pa)
P_{β}	pressure of phase β (Pa)
P_c	capillary pressure (Pa)
q_{β}	source/sink - or fracture matrix interaction of mass for phase β (kg/s m^3)
Q^{n+1}_{β}	source/sink or fracture-matrix exchange terms for phase β (kg/s) of time level n+1
R^{k}_{β}	residual term of mass balance of phase β (kg/m^3) of time level n+1
S_{β}	fluid saturation of phase β
t	time (s)
Δt	time step (s)
V_i	volume of gridblock i (m^3)
$\mathbf{v}_{\beta}$	Darcy's or volumetric velocity of phase β (m/s)
Z_i	depth of the center of blocki from a datum, m

Greek Symbols

α	Biot's effective parameter
β_{β}	effective non-Darcy flow coefficient for phase β (m^{-1}) of
ϕ	effective porosity of formation
Φ_{β}	flow potential (Pa)
γ_{ij}	transmissivity (m^3)
$\bar{\gamma}_{ij}$	transmissivity for non-Darcy flow (m^{-1})
$\lambda_{\beta,ij+1/2}$	mobility of phase β between gridblcoks i and j
μ_{β}	viscosity of phase β (Pa•s)
ρ_{β}	density of phase β at *in situ* conditions (kg/m^3)
σ_m	mean total stress (Pa)
σ'_m	mean effective stress (Pa)

Subscripts

0	zero stress condition
c	capillary
g	gas
i	gridblock i
j	gridblock j
β	index of fluid phase

Superscripts

0	zero stress condition
k	index for mass components.
n	previous time level n
n+1	current time level n+1
p	iteration level

References

Biot, M.A., General Theory of three dimensional consolidation, *J. Appl Phys*., 12: pp.57-64, 1941.

Bybee, K., Horizontal wells in tight gas sands: risk management to maximize success, *JPT*, 61-63, October, 2008.

Cippolla, C. L., E. P. Lolon, J. C. Erdle, and V. Tathed, Modeling Well Performance in Shale-Gas Reservoirs, Paper SPE 125532, presented at the 2009 SPE/EAGE Reservoir Characterization and Simulation Conference, Abu Dhabi, UAE, 19-21 October, 2009.

Denney, D., Rock type-understanding productivity in tight gas sands, *JPT*, 53-56, October, 2008.

Forsyth, P. A., Three-dimensional modeling of steam flush for DNAPL site remediation, *International Journal for Numerical Methods in Fluids, Vol.* 19 (1994), 1055-1081.

Forsyth, P. A., Y. S. Wu and K. Pruess, Robust Numerical Methods for Saturated-unsaturated Flow with Dry Initial Conditions in Heterogeneous Media. Advance in Water Resources 18, p. 25-38, 1995.

Kazemi, H., Pressure transient analysis of naturally fractured reservoirs with uniform fracture distribution. *Soc. Pet. Eng.*, 451-62, *Trans., AIME*, 246, 1969.

Kelkar M. and M. Atiq, Upgrading Method for Tight Gas Reservoirs, SPE 133301, presented at the SPE Annual Technical Conference and Exhibition, Florence, Italy, 19-22 September, 2010.

King, E. G., Thirty Years of Gas Shale Fracturing: What Have We learned?, SPE 133456, presented at the SPE Annual Technical Conference and Exhibition, Florence, Italy, 19-22 September, 2010.

Klinkenberg, L.J., The Permeability of Porous Media to Liquids and Gases, in API Drilling andProduction Practice, 200–213, 1941.

Lei, Qin, Wei Xiong, Jiangru Yuan, Yuquan Cui, and Yu-Shu Wu, "Analysis of Stress Sensitivity and Its Influence on Oil Production from Tight Reservoirs," SPE-111148, presented at the 2007 SPE Eastern Regional Meeting held in Lexington, Kentucky, U.S.A., 17–19 October 2007.

Leverett, M. C., Capillary Behavior in Porous Media, *Trans AIME*, 142:341-358, 1941.

MIT, The future of natural gas – an interdisciplinary MIT study, 2010.

Pruess, K., C. Oldenburg and G. Moridis, *TOUGH2 User's Guide, Version 2.0,* Report LBNL-43134, Berkeley, California: Lawrence Berkeley National Laboratory, 1999.

Pruess, K. and T. N. Narasimhan, A practical method for modeling fluid and heat flow in fractured porous media, *Soc. Pet. Eng. J.*, 25, 14-26, 1985.

Rutqvist, J. Y. S. Wu, C. F. Tsang, and G. S. Bodvarsson, A modeling approach for analysis of coupled multiphase fluid flow, heat transfer, and deformation in fractured porous rock, *International Journal of Rock Mechanics and Mining Sciences*, 39:429-442, 2002.

Pruess, K., C. Oldenburg and G. Moridis, *TOUGH2 User's Guide, Version 2.0,* Report LBNL-43134, Berkeley, California: Lawrence Berkeley National Laboratory, 1999.

Rutqvist, J. Y.S. Wu, C.F. Tsang, and G.S. Bodvarsson, A modeling approach for analysis of coupled multiphase fluid flow, heat transfer, and deformation in fractured porous rock, *International Journal of Rock Mechanics and Mining Sciences*, Vol. 39, 429-442, 2002.

Terzaghi, K., *Theoretical Soil Mechanics*, John Wiley & Sons Inc., New York, 1943.

Warpinski, N. R., M. J. Mayerhofer, M. C. Vincent, C. L. Cipolla, and E. P. Lolon, Stimulating Unconventional Reservoirs: Maximizing Network Growth While Optimizing Fracture Conductivity, presented at the 2008 SPE Shale Gas Production Conference, Fort Worth, Texas, 16-18 November, 2008.

Wu, Y.S. G. Moridis, B. Bai, and K. Zhang, A Multi-Continuum Model for Gas Production in Tight Fractured Reservoirs, SPE 118944, Prepared for presentation at the 2009 SPE Hydraulic Fracturing Technology Conference held in The Woodlands, Texas, USA, 19–21 January 2009.

Wu, Y.S. and G. Qin, A general numerical approach for modeling multiphase flow and transport in fractured porous media, *Communications in Computational Physics*, Vol. 6, No. 1, 85-108, July, 2009.

Wu, Y.S., J. Rutqvist, K. Karasaki, Q. Lei, W. Xiong, J. Yuan, M. Liu, and Y. Di, A mathematic model for rock deformation effect of flow in porous and fractured reservoirs," the 42nd US Rock Mechanics Symposium and 2nd U.S.-Canada Rock Mechanics Symposium, San Francisco, CA, 2008.

Wu, Y.S., L. Pan, and K. Pruess, A physically based approach for modeling multiphase fracture-matrix interaction in fractured porous media, *Advances in Water Resources*, Vol. 27, 875-887, 2004.

Wu, Y.S., Numerical simulation of single-phase and multiphase non-Darcy flow in porous and fractured reservoirs, *Transport in Porous Media*, Vol. 49, No. 2, 209-240, 2002

Wu, Y.S. A virtual node method for handling wellbore boundary conditions in modeling multiphase flow in porous and fractured media, *Water Resources Research*, 36 (3), 807-814, 2000.

Wu, Y. S. and K. Pruess, "Numerical Simulation of Non-Isothermal Multiphase Tracer Transport in Heterogeneous Fractured Porous Media," *Advances in Water Resources*, Vol. 23, 699-723, 2000

Wu, Y.S. and K. Pruess "A numerical method for simulating non-Newtonian fluid flow and displacement in porous media", Vol. 21, *Advances in Water Resources*, 351-362, 1998.

Wu, Y.S., K. Pruess, and P. Persoff, "Gas Flow in Porous Media with Klinkenberg Effects," *Transport in Porous Media*, Vol.32, 117-137, 1998.

Wu, Y. S., P. A. Forsyth and H. Jiang, A consistent approach for applying numerical boundary conditions for subsurface flow, *Journal of Contaminant Hydrology*, Vol. 23, 157-185, 1996.

Wu, Y. S., K. Pruess, and P.A. Witherspoon, "Flow and Displacement of Bingham Non-Newtonian Fluids in Porous Media," *SPE Reservoir Engineering*, pp.369-376, 1992

Wu, Y. S., and K. Pruess, A multiple-porosity method for simulation of naturally fractured petroleum reservoirs, *SPE Reservoir Engineering*, 3, 327-336, 1988.

Xiong, Wei, Qun Lei, Jiangru Yuan, Shusheng Gao, and Yu-Shu Wu, "Behavior of Flow through Low-Permeability Reservoirs," SPE-113144, prepared for presentation at the 2008 SPE EUROPEC Conference to be held in Rome, Italy, 9-12 June 2008

Table 1 – Input data for the simulation

Initial reservoir parameters		Rock mechanics properties	
Pressure (MPa)	32	Biot constant	0.8
Vertical stress (MPa)	70	Bulk modulus (MPa)	800
Horizontal stress (MPa)		Poisson ratio	0.2
Matrix porosity (fraction)	0.05		
Matrix permeability (m^2)	1E-16	**Production parameters**	
Fracture porosity (fraction)	0.005	Hydraulic fracture permeability (m^2)	0.9E-11
Fracture permeability (m^2)	1E-15	Fracture half length (m)	300
		Constant bottom hole pressure (MPa)	7

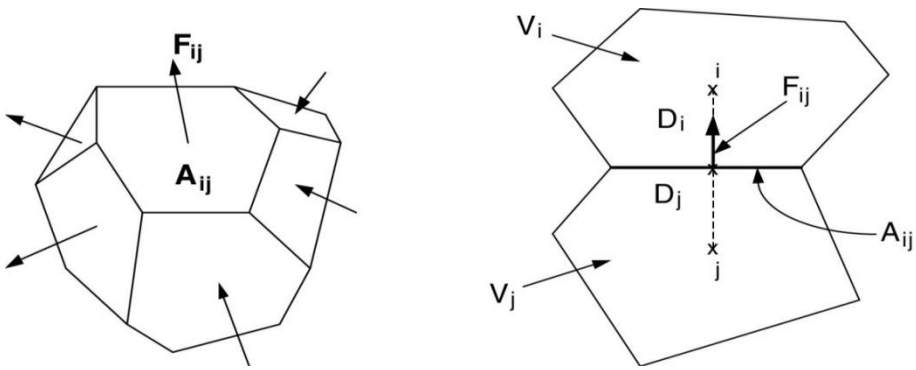

Fig. 1 – Space discretization and flow-term evaluation in the integral finite difference method (Pruess et al. 1999)

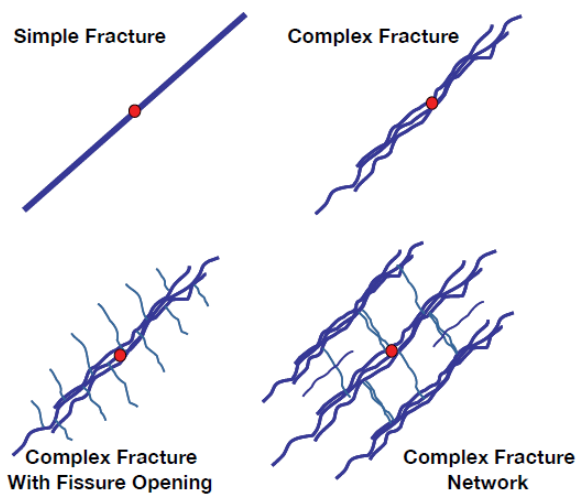

Fig. 2 – Schematic of the level of fracture complexities (Warpinski et al., 2008)

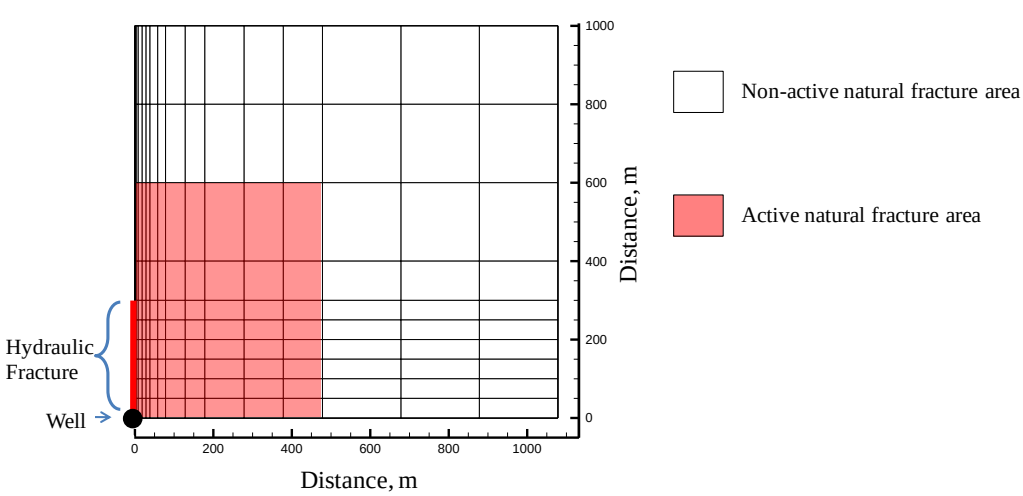

Fig. 3 – Configuration of a quarter of the hybrid fracture model of a hydraulically fractured reservoir system.

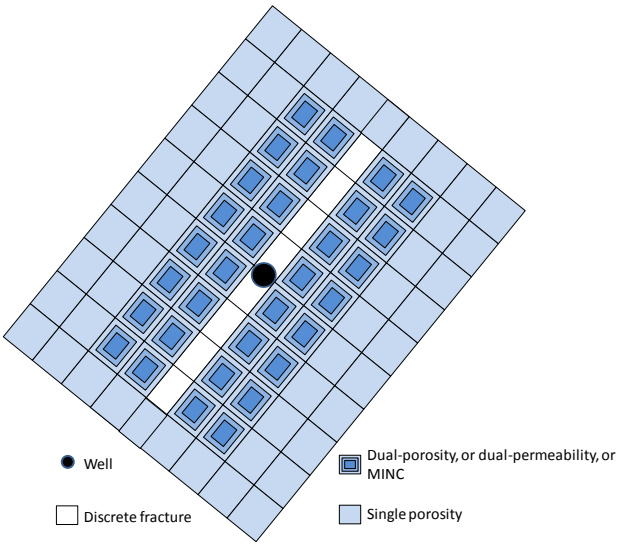

Fig. 4 – Schematic of a hybrid fracture model, coupling fluid flow and geomechanics for a hydraulically fractured reservoir system.

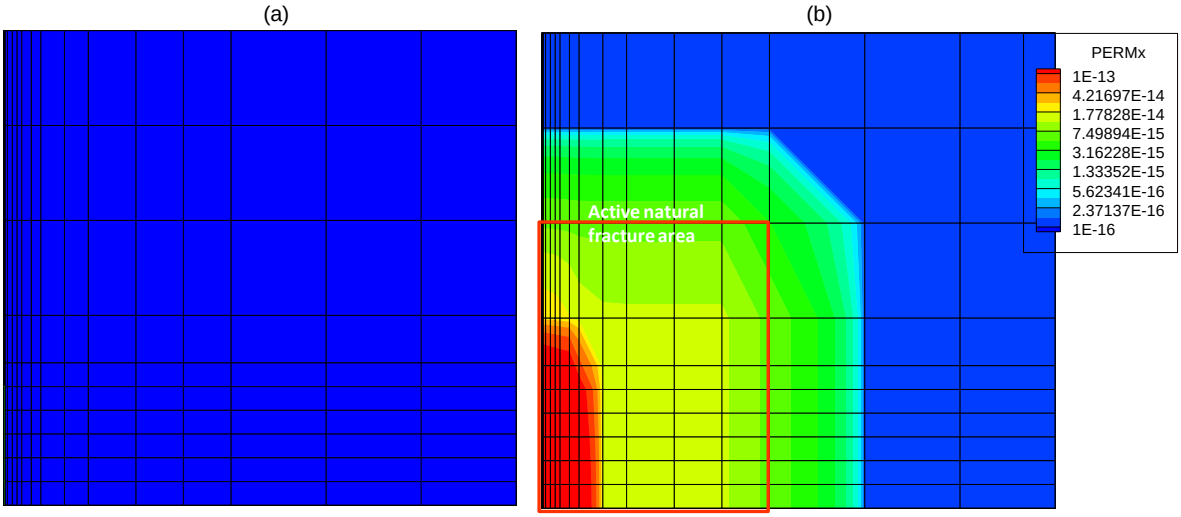

Fig. 5 – Permeability map (a) before, and (b) after a hydraulic fracturing treatment.

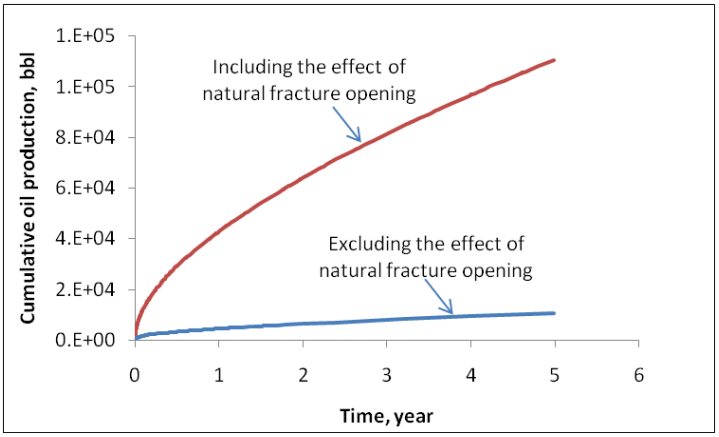

Fig. 6 – Cumulative oil production profiles: comparison between including and excluding the effect of natural fracture reopening.